Expression of Guanylyl Cyclase (GC)-A and GC-B during Brain Development: Evidence for a Role of GC-B in Perinatal Neurogenesis

Dieter Müller, Balanes Hida, Gabriela Guidone, Robert C. Speth, Tatyana V. Michurina, Grigori Enikolopov, and Ralf Middendorff

Institute of Anatomy and Cell Biology (D.M., B.H., R.M.), Justus-Liebig-University, 35385 Giessen, Germany; Institute for Hormone and Fertility Research (G.G.), University of Hamburg, 20251 Hamburg, Germany; Department of Pharmacology (R.C.S.), University of Mississippi, University, Mississippi 38677; and Cold Spring Harbor Laboratory (T.V.M., G.E.), Cold Spring Harbor, New York 11724

Atrial (ANP) and C-type (CNP) natriuretic peptide generate physiological effects via selective activation of two closely related membrane receptors with guanylyl cyclase (GC) activity, known as GC-A and GC-B. As yet, however, the discrete roles for ANP/GC-A *vs.* CNP/GC-B signaling in many mammalian tissues are still poorly understood. We here used receptor affinity labeling and GC assays to characterize comparatively GC-A/GC-B expression and functional activity during rat brain development. The study revealed that GC-B predominates in the developing and GC-A in the adult brain, with regional differences each between cerebral cortex, cerebellum, and brain stem. Whereas GC-A levels nearly continuously increase between embryonal d 18 and adult, GC-B expression in brain is highest and widely distributed around postnatal d 1. The striking perinatal GC-B peak coincides with elevated expression of nestin, a marker protein for neural stem/progenitor cells. Immunohistochemical investigations revealed a cell body-restricted subcellular localization of GC-B and perinatal abundance of GC-B-expressing cells in regions high in nestin-expressing cells. However, and supported by examination of nestin-GFP transgenic mice, GC-B and nestin are not coexpressed in the same cells. Rather, GC-B$^+$ cells are distinguished by expression of NeuN, an early marker of differentiating neurons. These findings suggest that GC-B$^+$ cells represent neuronal fate-specific progeny of nestin$^+$ progenitors and raise the attention to specific and pronounced activities of CNP/GC-B signaling during perinatal brain maturation. The absence of this activity may cause the neurological disorders observed in GC-B-deficient mice. **(*Endocrinology* 150: 5520–5529, 2009)**

The members of the natriuretic peptide (NP) family, atrial (ANP), B-type (BNP) and C-type (CNP) NP signal via binding to and stimulation of transmembrane receptors with guanylyl cyclase (GC) activity, resulting in intracellular accumulations of the second messenger, cGMP. ANP and BNP are cardiac hormones that use the same receptor, referred to as GC-A [also known as NP receptor (NPR)-A], for signal transduction (1, 2). In contrast, CNP operates in a paracrine/autocrine manner and is the specific agonist for GC-B (NPR-B) (1, 2).

The physiological impact of natriuretic peptide/GC/cGMP signaling in mammals is broad, ranging from regulation of blood pressure and fluid volume homeostasis (main target organs: vasculature, kidney, adrenal) to crucial effects exerted in a variety of other organ systems (1, 2). GC-A and GC-B are closely related proteins (3), and both are widely distributed among tissues (4, 5). Hitherto, only certain biological effects could be clearly assigned to either GC-A or GC-B signaling. These include the inhibition of adrenal aldosterone secretion (by ANP/

ISSN Print 0013-7227 ISSN Online 1945-7170
Printed in U.S.A.

doi: 10.1210/en.2009-0490 Received April 24, 2009. Accepted August 26, 2009.
First Published Online October 16, 2009

Abbreviations: Ad., Adult; ANP, atrial natriuretic peptide; BNP, B-type natriuretic peptide; CNP, C-type natriuretic peptide; CNPase, 2′, 3′-cyclic nucleotide 3′-phosphodiesterase; CNS, central nervous system; DAPI, 4′,6-diamidino-2-phenyl-inodole; E, embryonic day; GC, guanylyl cyclase; GFAP, glial fibrillary acidic protein; GFP, green fluorescent protein; IR, immunoreactivity; NeuN, neuronal nuclei; NF-H, neurofilament H; nNOS, neuronal NO synthase; NO, nitric oxide; NP natriuretic peptide; NPR, NP receptor; P, postnatal day.

GC-A) (6, 7) and the regulation of bone growth by CNP/GC-B (8, 9).

The brain is one of the NP target tissues where the specific roles for GC-A and GC-B are poorly understood. Based on examinations at the mRNA level and by receptor autoradiography (reviewed in Ref. 10), NPs and their receptors seem present and widely distributed in the central nervous system (CNS). Signaling by NPs has been linked to neuronal functions such as neurotransmitter release, synaptic transmission, axonal branching, neuroprotection, and neuroendocrine regulation (10, 11). Highlighting an additional aspect of physiological significance, there is accumulating evidence that natriuretic peptides play roles during brain development (10, 12). Corresponding data include the demonstration of discrete NP and receptor gene expression patterns in the embryonic brain (13). Functionally, there is evidence that NP-GC-cGMP signaling controls axonal bifurcation and pathfinding during nervous system development (14) and promotes the differentiation of olfactory neuronal precursor cells (15). Assessments of postnatal time courses of ANP and CNP gene expression (16) revealed transiently elevated expression levels in different rat brain regions, further supporting NP functions in developmental processes. As yet, analogous investigations of GC-A and GC-B, responsible for mediating the cellular effects of ANP and CNP, have not been reported. In addition, discrepancies between gene expression analyses and data derived by receptor autoradiography suggested the existence of NP-interacting proteins structurally different from the known NPRs (12). Thus, experimental efforts to characterize unambiguously these receptors in brain were desirable.

The present investigation aimed to resolve the expression profiles of GC-A and GC-B in the developing and adult rat brain. To characterize the native proteins in a conclusive manner, we used complementary approaches involving receptor detection at the molecular level by affinity labeling and assessments of their agonist-dependent enzyme activities. These studies revealed a directly opposed postnatal developmental regulation of the two cGMP-generating NPRs. The resulting strong expression of GC-A in the adult brain suggests a predominant activity of this receptor in terminally differentiated cell types of the mature CNS. In contrast, an intriguing perinatal expression peak of GC-B, coinciding with transiently elevated expression of the neuroepithelial stem/progenitor cell marker protein nestin (17, 18), pointed at functions for GC-B in the context of proliferation and/or maturation of neural progenitor cells. Immunohistochemical investigations revealed mostly overlapping regional distribution patterns of nestin$^+$ and GC-B$^+$ cells but no coexpression of the two antigens in individual cells. Coexpression of GC-B with neuronal nuclei (NeuN), a neuron-specific nuclear antigen that marks maturing and differentiated neurons (19), indicates a dynamic role for CNP/GC-B signaling in neurogenesis with highest impact during perinatal development.

Materials and Methods

Materials

The synthetic peptides ANP (residues 1-28, rat) and CNP (residues 32-53, rat) were purchased from Bachem (Weil am Rhein, Germany), ^{125}I-ANP (IM 186; 2 kCi/mmol) from Amersham (Freiburg, Germany). ^{125}I-[Tyr^0]CNP32-53, 2.2 kCi/mmol, was prepared at the Peptide Radioiodination Service Center (University, MS). 1-Methyl-3-isobutyl xanthine was from Sigma (Taufkirchen, Germany) and protease inhibitors were from Roche (Mannheim, Germany).

Animals and tissues

Wistar rats (Charles River Laboratories, Sulzbach, Germany) of different developmental stages were dissected after decapitation, and the tissues were immediately frozen in liquid nitrogen and stored at −80 C. Embryonic brains (n = 4–6 each) were pooled before homogenization. Embryonic and postnatal day (P) 1 brains, unless otherwise specified, were derived from both males and females. All other rat tissues were from male animals. Nestin-green fluorescent protein (GFP) transgenic mice were described previously (20). The animals were used according to government principles regarding the care and use of animals with permission (G8151/591-00.33) of the local regulatory authority.

Preparation of membrane and soluble protein fractions

Protein fractions were prepared as described (21). In brief, frozen tissues were pulverized in a mortar and then homogenized using a Potter-Elvehjem homogenizer. After centrifugation at 3,000 × *g* to remove cell debris and nuclei, proteins were separated into soluble and particulate (membrane) fractions by centrifugation at 100,000 × *g*. Protein concentrations were determined by using a kit from Bio-Rad (Munich, Germany) with BSA (Sigma; fraction V) as standard.

Receptor affinity labeling

Protocols for photoaffinity labeling of natriuretic peptide receptors in crude membranes by ^{125}I-ANP (4) or ^{125}I-[Tyr^0]CNP (22) have been reported before. In brief, membranes were incubated with radiolabeled ANP (0.5 nM) or CNP (2 nM), ligand/receptor cross-links were induced by UV light irradiation, and reaction products were analyzed by SDS-PAGE under reducing conditions in 7.0% acrylamide separation gels followed by autoradiography at −70 C using XAR-5 film (Kodak, Rochester, NY) and intensifying screens. Radiolabeled receptors, excised from dried gels, were quantified in a BF 5300 γ-counter (Berthold, Bad Wildbad, Germany).

Assay of particulate (membrane) GC activity

The protocol for determination of basal and NP-stimulated GC activity in crude membrane preparations has been published

before (23). Assays were performed for 12 min in either the absence or presence (1 μM) of ANP or CNP, respectively, and reactions were started by addition of 10 μg of membrane protein. Measurements of cGMP by a commercial ELISA (IHF, Hamburg, Germany) were described previously (4).

Immunoblotting

After separation by SDS-PAGE under reducing conditions, proteins were transferred to nitrocellulose membranes as specified before (23). Blots were stained with Ponceau S (P7170; Sigma), and the protein images were used to control protein loading. After blocking (23), blots were exposed to antibodies directed against GC-A (PGCA-101AP; Fabgennix, Frisco, TX), GC-B (PGCB-201AP; Fabgennix), nestin (MAB 353; Chemicon, Temecula, CA), neuronal nitric oxide synthase (nNOS; 610308; BD Biosciences, San Jose, CA), neurofilament-H (NF-H, NA 1209; Biotrend, Köln, Germany), glial fibrillary acidic protein (GFAP; G3893; Sigma), or 2′, 3′-cyclic nucleotide 3′-phosphodiesterase (CNPase; MAB 326R; Chemicon). After incubation with goat antirabbit or antimouse IgG (Pierce, Rockford, IL), linked to peroxidase, signals were detected via enhanced chemiluminescence (23).

Immunofluorescence

Brains from P1 Wistar rats were removed en block and treated overnight with 4% paraformaldehyde in PBS, followed by incubation for 24 h in 18% sucrose in PBS. Organs were embedded in Tissue-Tek OCT compound (Sakura, Zoeterwoude, The Netherlands), frozen in liquid nitrogen, and cut into 10-μm sections. After blocking of unspecific protein binding sites by 2% normal goat serum (Sigma) in PBS, the sections were incubated overnight with anti-GC-B (FabGennix; 1:50), anti-GFAP (Sigma; 1:1000), antinestin (Chemicon; 1:100), and/or anti-NeuN (MAB 377; Chemicon; 1:100) followed by simultaneous exposure to Cy3-conjugated goat antirabbit IgG (Jackson ImmunoResearch, West Grove, PA; 1:500), Alexa Fluor 488 goat antimouse IgG (Molecular Probes, Eugene, OR; 1:1000), and 4′,6-diamidino-2-phenyl-inodole (DAPI; 1 μg/ml) for 1 h at room temperature. Sections, in which primary antibodies were omitted, served as controls. Images were obtained by conventional fluorescence microscopy (Axioskop 2; Zeiss, Oberkochen, Germany) or confocal laser scanning microscopy (TCS SP5; Leica, Wetzlar, Germany).

Nestin-GFP transgenic mice of P1 were fixed with 4% paraformaldehyde/PBS for 7 h and then placed into 30% sucrose/PBS for 2 d. Brains were removed and embedded in Tissue-Tek (see above). For detection of GFP fluorescence (24) and simultaneous immunofluorescence analyses (see above), 10-μm sections were used.

Experimental reproducibility and data analysis

All results shown were representative of at least three independent experiments performed. For densitometric quantification, ImageJ (open source; NIH, Bethesda, MD) was used. Data were graphed and analyzed using Prism 3.02 (GraphPad Software Inc., San Diego, CA). The significance of effects was assessed using Student's *t* test.

Results

Assessment of NPR expression by photoaffinity labeling

Rat pineal gland membranes, characterized previously by exceptionally high expression levels of GC-B (22), were used in initial experiments to judge and optimize experimental conditions for photoaffinity labeling of this receptor. Based on a more than 10-fold reduced affinity of iodinated forms of Tyr^0-CNP for GC-B (25), the sensitivity of GC-B detection by the photoaffinity labeling approach is markedly lower than that of analogous GC-A detection assays with iodinated ANP. The specific labeling of GC-B by ^{125}I-Tyr^0-CNP after UV light irradiation (supplemental Fig. S1, published as supplemental data on The Endocrine Society's Journals Online web site at http://endo.endojournals.org), and the results of experimental efforts to increase the yield of GC-B labeling (supplemental Fig. S2) are shown. Further studies served to prove the receptor-specificity (GC-A *vs.* GC-B) of the photoaffinity labeling approach (supplemental Fig. S3).

GC-A and GC-B are differentially regulated during development in brain

To examine comparatively GC-B and GC-A expression during brain development, membrane preparations from rat brains of different embryonic day (E; 18 and 20), postnatal (P1-28), and adult (Ad., 3 months) stages were incubated with either ^{125}I-Tyr^0-CNP or ^{125}I-ANP before UV light-induced ligand/receptor cross-linking, and reaction products were analyzed by SDS-PAGE and autoradiography. These studies revealed a massive increase in GC-A expression during ontogeny (Fig. 1A). As calculated by γ-counting of the excised radiolabeled receptor bands, this increase was 20-fold between E18 and adult. Comparing P1 and adult, the increase was 6-fold.

A completely different developmental regulation was observed in the case of GC-B. This receptor was detectable only at early developmental stages, with a pronounced expression peak at P1 (Fig. 1B). Considering the abovementioned reduced sensitivity of GC-B detection by the photoaffinity labeling approach, these findings clearly revealed strikingly high perinatal levels of GC-B in brain but could not be used to predict an absence of GC-B expression at later developmental stages.

Immunoblot analyses were consistent with the photoaffinity labeling data and confirmed the decrease in GC-B (and the increase in GC-A) levels between P1 and adult (Fig. 1C). As specificity controls, we coexamined receptor expression in membranes from rat adrenal, representing a major GC-A expression site (4) and pineal gland, an outstanding GC-B expression site (22). These studies in addition corroborated a previously reported size

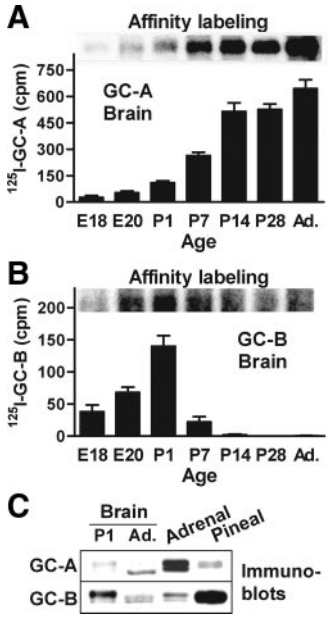

FIG. 1. Developmental regulation of GC-A and GC-B. A, Rat brain membranes (50 μg protein) derived from different embryonic (E18 and E20) or postnatal (P1-28; Ad., 3 months old) stages were incubated with ^{125}I-ANP, ligand/receptor cross-links were induced by UV irradiation, and reaction products were analyzed via SDS-PAGE and autoradiography. The resulting radiolabeled ANP receptor (GC-A) bands are shown at the *top*. For quanitification, receptor bands were excised from the dried gels, and the amounts of radioactivity were measured by γ-counting. The graph shows the mean ± SE of four experiments. B, The same experiments as in A were performed with ^{125}I-Tyr^0-CNP instead of ^{125}I-ANP. Radiolabeled GC-B bands from a representative experiment (*top*) and the quantitative evaluation of four experiments are shown. C, Immunoblots comparing levels of GC-A (*upper panel*) or GC-B (*lower panel*) in equal amounts (60 μg) of membrane protein from rat brain (P1 *vs.* Ad.), adrenal, and pineal gland (adult each).

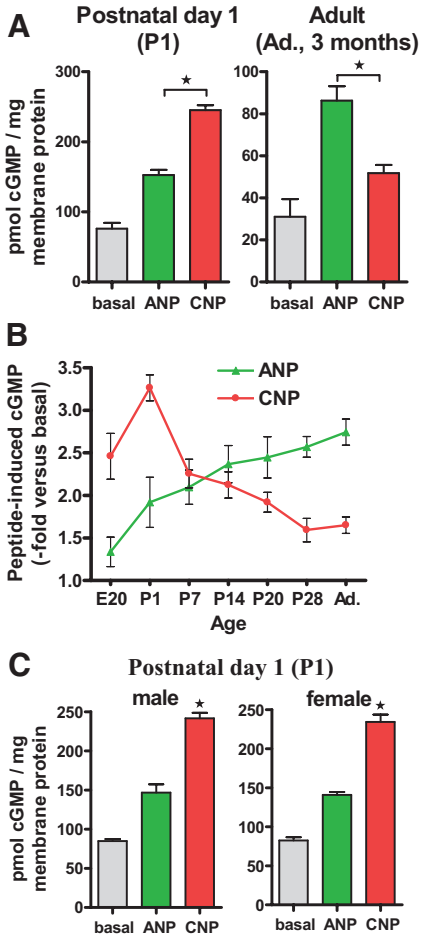

FIG. 2. ANP- and CNP-dependent cGMP production by brain membranes from different developmental stages. A, Production of cGMP in the absence (basal) or presence (1 μM) of ANP or CNP by brain membranes (10 μg protein) from either neonatal (P1) or adult animals. Amounts of cGMP were determined by ELISA. The data represent the mean ± SE of four independent experiments each. *, $P < 0.005$ *vs.* ANP (P1) or CNP (Ad.). B, Basal and ANP- and CNP-induced cGMP production by brain membranes (10 μg protein) from different developmental stages (indicated) was measured as in A. Values obtained in the presence of the peptides were divided through the yields of cGMP measured in the absence of agonists each and expressed as fold stimulation *vs.* basal. Data shown are mean ± SE of three separate experiments. C, Production of cGMP in the absence (basal) or presence (1 μM) of ANP or CNP by P1 brain membranes (10 μg protein) from either male or female rats. Amounts of cGMP were determined by ELISA. *, $P < 0.001$ *vs.* ANP, n = 4 each. There are no significant differences between male and female cGMP levels.

shift (*i.e.* a decrease in kilodaltons) of GC-A during postnatal brain development (4).

We next investigated comparatively, by GC assays, the agonist-dependent enzymatic activities of GC-A and GC-B in perinatal and adult brain. Consistent with the protein expression data, the GC-B ligand, CNP, generated higher cGMP accumulations than ANP (acting on GC-A) at P1 membranes, whereas ANP was the more effective peptide in the case of adult membranes (Fig. 2A). With maximal 3.3-fold (CNP at P1) and 2.8-fold (ANP at adult brain membranes) increases in GC activity, the peptide-elicited effects were limited. In our experience, a restricted sensitivity to agonist stimulation is typical for membrane preparations, from either native tissues or cell lines endogenously expressing NPRs (26). Several experimental efforts to enhance GC stimulation by the receptor ligands remained unsuccessful. Neither the addition of phosphatase inhibitors (to prevent dephosphorylation/desensitization of GC-A and GC-B) during tissue homogenization (supplemental Fig. S4) nor the presence of protease inhibitors during peptide exposure (bacitracin, up to 2 mg/ml; data not shown) could markedly elevate ligand-dependent GC activities. Also, cGMP production did not differ significantly between freshly prepared (never frozen) membranes and membranes after storage at −80 C (supplemental Fig. S5). Thus, disruption of the cellular plasma membrane topology during homogenization might essentially contribute to reduced agonist sensitivity.

As disclosed by assays with brain membranes from different developmental stages, GC-B activity predominates before birth and postnatally at least until P7 (Fig. 2B). GC-A-mediated cGMP production begins to exceed that

of GC-B between P7 and P14 (Fig. 2B). Remarkably, basal GC activities are much higher at P1 than in the adult brain (see Fig. 2A). A detailed analysis, indicating to what extent this activity varies during development, is shown (supplemental Fig. S6).

Basal as well as ANP- and CNP-elicited cGMP accumulations did not differ between brain membranes derived from males or females at P1 (Fig. 2C), indicating that the high perinatal GC-B expression is a gender-independent phenomenon.

High GC-B expression in brain at P1 is widely distributed and most prominent in the cerebral cortex

We next questioned whether the abundant GC-B expression around birth, observed in whole brain tissue, is based on a broad receptor distribution or due to high concentrations in only a subset of brain areas. GC assays with membranes from isolated cerebral cortex, cerebellum, and brain stem (Fig. 3A) demonstrated that CNP is highly effective and more potent at generating cGMP than ANP in all three areas at P1. Thus, GC-B is widely distributed in brain after birth and represents the predominant NPR

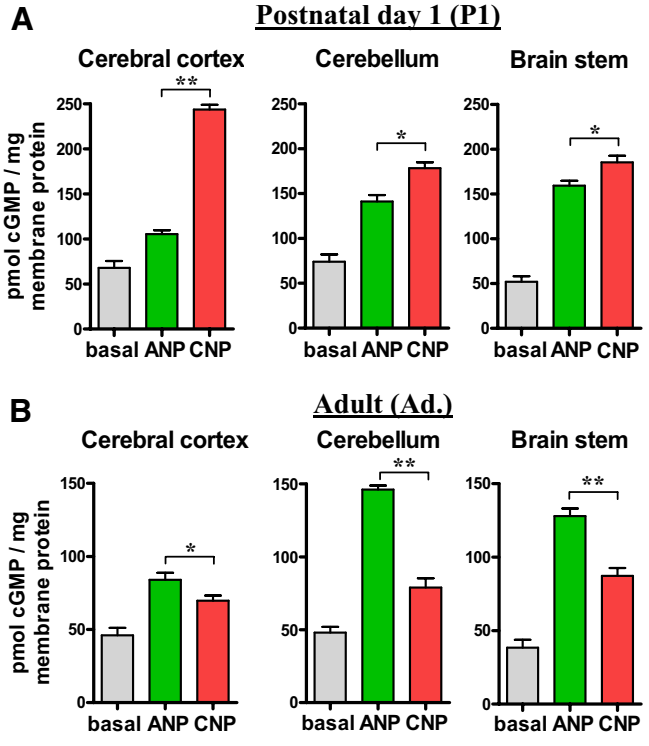

FIG. 3. GC assays with membranes from different brain regions. A, Assessment of basal and ANP- and CNP-dependent cGMP production by membranes from the P1 brain regions indicated. CNP elicits significantly (**, $P < 0.001$; *, $P < 0.05$) more cGMP than ANP in all regions (n = 3 each). B, Basal and ANP- and CNP-dependent cGMP production by membranes from different Ad. brain regions. ANP is more effective than CNP (**, $P < 0.001$; *, $P < 0.05$) in raising cGMP levels (n = 5 each).

in each one of the regions examined. This investigation also revealed that cerebral cortex is distinguished by both the highest levels of GC-B and the lowest levels of GC-A activity at P1. Analogous assays with membrane preparations from adult animals showed (Fig. 3B) that ANP was more effective than CNP to generate cGMP. Highest levels of GC-A activity were found in cerebellum and brain stem membranes. By comparing the alterations between P1 and adult, GC-B-mediated cGMP formation decreases most significantly in the cerebral cortex, and GC-A-mediated cGMP formation increases most vigorously in cerebellum.

The perinatal expression peak of GC-B coincides with nestin (a marker for neural stem/progenitor cells) expression

Taking into account the abundant and widespread expression of GC-B in whole brain tissue at P1, indicating quantitatively significant amounts of GC-B expressing cells, we examined by immunoblot analyses the expression levels of proteins representing marker molecules for different cell types in the brain. These experiments demonstrated an only very poor expression at P1 of cell type-specific markers for terminally differentiated neurons (NF-H), oligodendrocytes (CNPase) and astrocytes (GFAP) in either soluble or particulate brain protein fractions (Fig. 4A). As expected, these proteins are abundant in the adult brain. Analogous examinations of nNOS, which is expressed in developing and differentiated neurons (27), revealed a substantial expression at P1 and a less pronounced increase in adult tissue (Fig. 4A).

These findings focused the attention on cells acting as progenitors for the differentiated cell types of the mature brain. Corresponding analyses of nestin, a marker for neuroepithelial stem cells (17, 18), revealed a perinatal (from E20 to P14) developmental expression profile (Fig. 4B), in part reminiscent of that of GC-B (Fig. 1B). Although nestin levels were more abundant at E18 than at P1, consistent with observations in nestin-GFP transgenic mice that overall nestin expression is highest in the developing brain between E14 and 15 (20), we observed a decrease from E18 to E20 before the formation of a subsequent expression peak around birth (Fig. 4C). The correlation of the latter with the perinatal GC-B expression peak disclosed a temporally confined (around birth) developmental stage during which transient increases in neural progenitor cell activity (deduced from nestin expression) and GC-B expression coincide.

The appearance of additional nestin-immunoreactive bands (Fig. 4B) likely represents nestin degradation products, which are typically seen in such analyses (28). Regarding the apparent molecular mass of nestin, usually estimated from the positions of comigrated size marker proteins, some previous studies (24, 29) assessed values

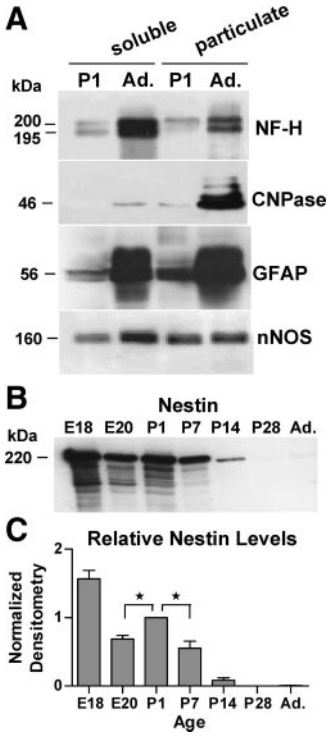

FIG. 4. Immunoblot analyses of marker proteins for neural cell types. A, Soluble and particulate (60 μg protein each) fractions of brain homogenates from either P1 or Ad. rats were examined by immunoblotting for NF-H, CNPase, GFAP, and nNOS. Protein sizes (in kilodaltons), calculated from comigrated reference proteins, are shown. B, Immunoblot for nestin of soluble rat brain proteins (20 μg) from different embryonic (E18 and E20) and postnatal (P1-28) developmental stages including Ad. (3 months). C, Densitometric quantification of nestin levels. Data are from three independent immunoblot analyses. For each blot, densitometry scores were normalized to the value obtained for nestin expression at P1. *Bars*, Mean scores ± SE in relation to those for P1 (set as 1). Nestin levels at P1 were significantly (*, $P < 0.05$) higher than those at E20 and P7.

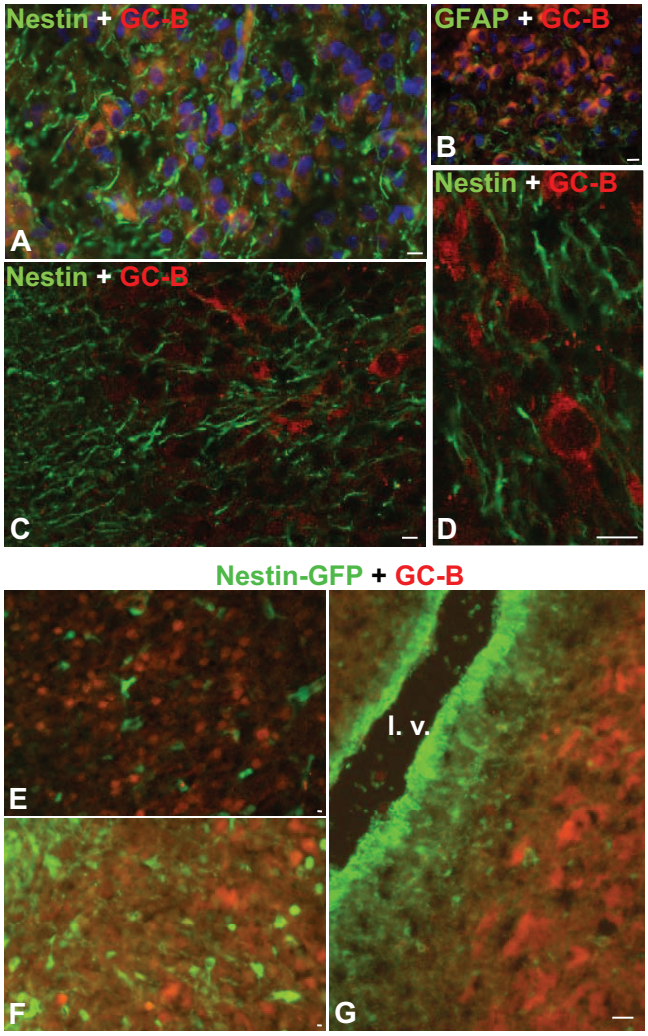

FIG. 5. GC-B- and nestin-expressing cells in P1 brain. A, C, and D, Codistribution of nestin and GC-B IR. Nestin-positive fibers and GC-B-positive perikarya are present in areas of the neonatal rat cerebral cortex (A) and brain stem (C and D) in close proximity (A: fluorescence microscopy, nuclei are stained with DAPI; C and D: confocal microscopy). B, GC-B and GFAP IR. GFAP, poorly detectable at P1, is visible in certain distance to GC-B$^+$ cells near the surface of the frontal cortex. DAPI marks nuclei. E–G, Visualization of nestin-GFP and GC-B IR in different regions of the P1 cerebral cortex (E and F) and close to the lateral ventricle (l.v.; G) from nestin-GFP transgenic mice. Sites of coexpression (would appear in *yellow*) are undetectable (E: shorter exposure times to focus on GFP$^+$ nuclei; F: longer exposure time to visualize both cell bodies and processes). *Bars*, 20 μm.

(~440 kDa) obviously incompatible with the expected molecular weight of 200,000 by cDNA analysis (17). We addressed this discrepancy by analyzing identical samples in different gel systems and found (data not shown) an anomalous (*i.e.* retarded) gel migration behavior of nestin at low (≤6%) acrylamide concentrations.

Nestin- and GC-B-expressing cells are in close proximity

The high perinatal (P1) expression levels of GC-B suggested a considerable frequency of GC-B-expressing cells at that stage. This was confirmed by immunohistochemical investigations. Examinations of P1 rat brain sections revealed large amounts and a broad distribution of GC-B$^+$ cells in the cerebral cortex as well as a predominantly cell body-localized receptor immunoreactivity (Fig. 5, A and B). Consistent with analyses of GC-B enzyme activity (Fig. 3), GC-B$^+$ cells were less abundant in brain stem (Fig. 5C) and cerebellum (not shown). As expected, there was a broad and massive expression of nestin in P1 brain (Fig. 5, A and C). Compared with nestin, GFAP was poorly detectable and showed a much more restricted regional distribution, for the most part at brain surface areas (Fig. 5B). GC-B$^+$ and nestin$^+$ cells were in close proximity in all brain regions (Fig. 5, A and C). Locally the ratio of GC-B$^+$ to nestin$^+$ cells in such regions varied appreciably, ranging from areas with a great excess of nestin$^+$ cells to those in which GC-B$^+$ cells were accumulated (Fig. 5, A and C). Enhanced resolution by confocal microscopy confirmed the mostly perikarya localization of GC-B and revealed a

punctual appearance of receptor immunoreactivity (IR) (Fig. 5, C and D).

The overlapping distribution of nestin and GC-B IR raised the possibility of cells that coexpress both antigens. Due to the different subcellular localization of nestin (cell processes) and GC-B (perikarya), corresponding clear-cut assessments by double-labeling studies were difficult. To circumvent this handicap, we used nestin-GFP transgenic mice based on findings that GFP in these animals is detectable also in the nuclei of nestin-expressing cells (20). Examinations of P1 brains demonstrated abundant occurrence of GC-B$^+$ cells also in mice and provided convincing evidence for the absence of cells that coexpress nestin and GC-B (Fig. 5, E–G). Remarkably, the periventricular surfaces, known sites of particularly high concentrations of nestin (20, 30), are devoid of GC-B IR. Accumulations of GC-B$^+$ cells were detectable at different distances to the ventricular zones (Fig. 5G).

GC-B$^+$ cells at P1 are characterized by NeuN expression

The above distribution and coexpression analyses suggested that GC-B$^+$ cells may represent progeny of nestin$^+$ progenitor cells. Because nestin expression decreases when cells proceed toward neuronal differentiation (20), we examined the expression of NeuN, a neuron-specific and mainly nuclear protein thought to represent an early marker of neuronal differentiation (19). These investigations revealed that GC-B$^+$ cells are characterized by NeuN expression (Fig. 6). Whereas all GC-B$^+$ cells were NeuN positive, the degree of GC-B IR associated with NeuN$^+$ cells varied strongly between individual cells, and major amounts of NeuN$^+$ cells without detectable GC-B expression were evident (Fig. 6A). Interestingly, the NeuN/GC-B coexpressing cells seemed to be distinguished by a higher-than-average intensity of NeuN IR and the appearance of perinuclear in addition to nuclear staining (Fig. 6, B–E). There is also evidence that GC-B and NeuN IR can extend a certain distance into cell processes (see *inset* in panel A and panel D).

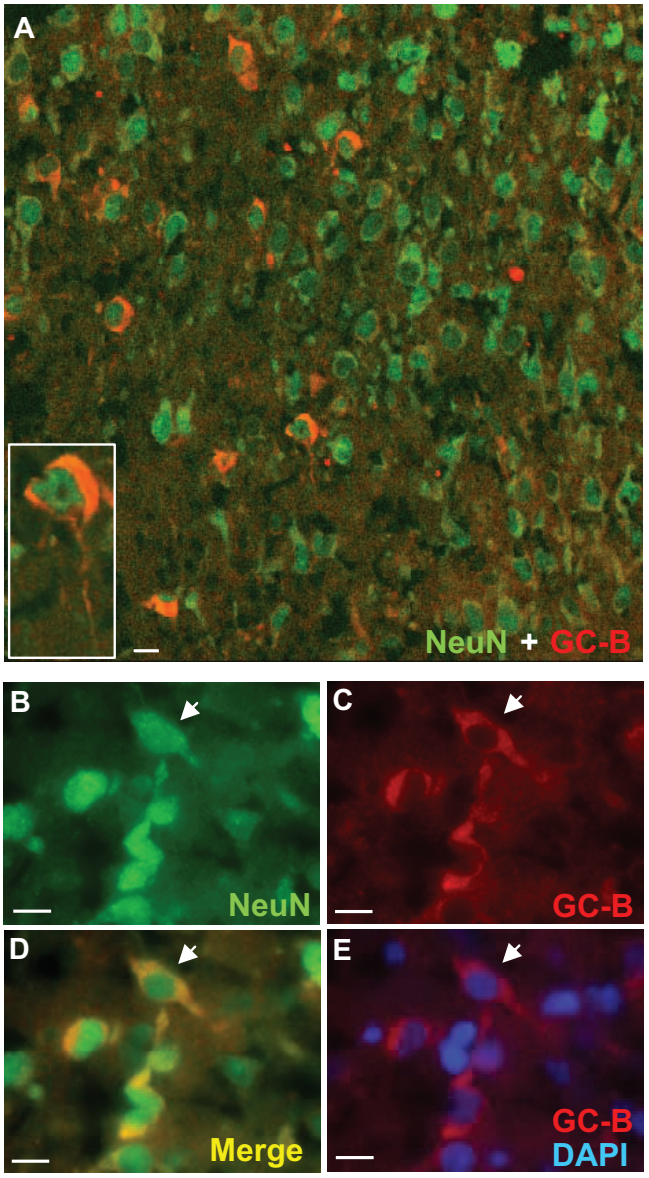

FIG. 6. Coexpression of GC-B and NeuN in P1 brain. A, Nerve cells, stained by NeuN, in a representative region of the cerebral cortex in P1 rat brain (confocal microscopy). NeuN is predominantly visible in cell nuclei. Neurons coexpressing NeuN and GC-B are easily detectable. The *inset* shows one of these cells at higher magnification. Note the GC-B-positive neurite. B–E, Magnification of an area in which NeuN/GC-B-coexpressing cells reside (fluorescence microscopy). B, NeuN IR is detectable with different staining intensity between individual cells and is not exclusively restricted to the nuclei (see D and E; note especially the cell marked by an *arrow*). C, Visualization of perikarya-localized GC-B IR. D, *Yellow color* marks sites of NeuN/GC-B coexpression in the cytoplasm. E, Visualization of GC-B IR and cell nuclei by DAPI. *Bars*, 20 μm.

Discussion

NPR expression in the developing and adult brain

Expression of GC-A in brain tissues was well verifiable by affinity-labeling experiments. Previous comparative examinations of GC-A levels in different central and peripheral rat tissues (4) have shown that the early postnatal brain represents an exceedingly poor GC-A expression site *in vivo*. The possibility to visualize the even lower concentrations of this receptor in prenatal brain tissues demonstrates the high sensitivity and favorable usability of this approach. Representing a further advantage of the affinity labeling approach, ^{125}I-ANP binds and becomes covalently linked to both GC-A (120–130 kDa) and a third NPR, NPR-C, of 60 kDa (23). Expression of NPR-C is seen by such experiments in diverse tissues, ranging from testis and fat (23) to lung, kidney, and choroid plexus (data not shown). However, and as demonstrated before (4),

NPR-C expression remained undetectable in both early postnatal and adult brain membranes. These findings suggest that NPR-C does not play a major role during brain maturation. In addition, our study failed to provide evidence for a discussed (12) potential existence of atypical ANP receptors in brain.

Detection of GC-B by affinity-labeling with ^{125}I-Tyr^{0}-CNP, despite the positive effect induced by inclusion of 0.1% sodium dodecyl sulfate (supplemental Fig. S2) remained restricted to tissues with exceptionally high receptor levels. In addition to the perinatal brain, adult pineal glands, and pituitaries (22) represent such tissues.

The exceptionally high expression of GC-B at P1 was confirmed by immunoblot analyses and GC assays, and these approaches allowed to assess the expression of the receptor also in the adult brain. We recognized some notable region-specific peculiarities. The cerebral cortex was found to be distinguished by the highest expression of GC-B at P1 and poor expression levels of both receptors in the adult. Consistently, the cerebellum and brain stem turned out to be the major sites of GC-A expression within the adult brain. These data suggest that the cerebral cortex is a key target tissue for CNP during perinatal development and indicates particularly pronounced signaling activities of ANP within the adult cerebellum and brain stem.

Because ANP- and CNP-stimulated cGMP production by P1 brain membranes was indiscriminative between males and females, there was no evidence for gender-related differences in perinatal NP receptor expression.

It should be noted that we did not find a quantitative correlation between receptor levels and their agonist-dependent cGMP production. Whether the perikarya localization of GC-B, proposed alterations in GC-A glycosylation during brain development (4) and/or developmental changes in the amount of receptor phosphorylation (and hence activity) are involved, remains to be addressed.

Perinatal abundance of GC-B in brain and coincidence with nestin expression

The high levels of GC-B (but not GC-A) in the embryonic and early postnatal brain suggested specific functions for CNP signaling in brain development. In support of this, CNP gene expression was detectable in mouse brain already at the onset of neurogenesis (E10.5) and increased further 4 d later, whereas ANP (and BNP) transcripts remained undetectable in embryonic brain (13). The high levels of GC-B protein (Fig. 1B) and CNP-dependent GC-B activity (Fig. 2B) at the late embryonic stages (E18 and E20), each exceeding those in the adult brain, suggests that GC-B is present and active even at earlier embryonic stages including the beginning of neurogenesis. However, the pronounced peak of GC-B expression around P1 indicates a maximum activity at the perinatal period.

The strikingly similar developmental expression profiles of GC-B and nestin between E20 and P14 suggested either a synchronized functional interrelationship between nestin-expressing neural stem/progenitor cells and GC-B-expressing cells and/or the existence of cell populations with coexpression of these proteins. In any case, these findings endorsed a role for CNP in processes of neurogenesis.

Characterization of GC-B^{+} cells

Immunohistochemical investigations revealed high amounts of GC-B IR in the perinatal brain and elucidated a major perikarya localization of the receptor. Consistent with the results of GC assays (Fig. 3A) and supporting signal specificity, the overall occurrence of GC-B IR was most prominent in the cerebral cortex. Further validation derived from immunohistochemical investigations on rat aorta sections, in which GC-B IR was found to be localized to the known sites (endothelial and vascular smooth muscle cells) of GC-B expression, and from Western blot analyses (Fig. 1C) with the same antibody. Analogous examinations performed with anti-GC-A did not show GC-B-comparable IR, and the only detectable staining at P1 was localized to blood vessels. On adult brain sections, GC-A IR was prominent on processes (*e.g.* axons) of mature neurons (not shown).

GC-B^{+} cells were codistributed with sites of nestin expression, supporting the idea of a functional interrelation including the possibility of coexpression at the cellular level. To be able to address the latter question in a conclusive manner by double-labeling experiments, we made use of nestin-GFP transgenic mice, in which nestin-expressing cells are labeled by GFP also in the nuclear compartment (20). These studies negated the existence of cells that coexpress the two proteins and raised the attention to progeny of nestin^{+} cells. The overlapping distribution patterns of nestin and GC-B IR, and the observation of areas in which either nestin- or GC-B-expressing cells predominate, were indicative of such an interrelation. The pronounced perinatal expression peak of GC-B suggests a transient emergence of a relatively abundant cell population with pronounced GC-B expression. This process might be even more dynamic if one considers the heterogeneous distribution (and varying relative accumulation) of these cells and their presumed nestin-expressing progenitors. Thus, at the single-cell level, there should be a markedly rapid turnover of GC-B expression. During the onset of GC-B expression, large amounts of maturing (intracellular) GC-B precursors should be detectable under such conditions. On the other hand, the subsequent decrease in GC-B expression might involve receptor inter-

nalization/endocytosis events, which also favors the occurrence of intracellular immunoreactivity. In apparent support of these theoretical considerations, enhanced resolution by confocal laser-scanning microscopy (Fig. 5D) revealed a punctual appearance of intracellular GC-B.

Consistent with other investigations (20, 30), we found that nestin expression at P1 is highly accumulated in cell layers surrounding the ventricles. However, in both nestin-GFP mice and rats, we saw a broad and significant expression of nestin in other cortical areas, brain stem and cerebellum at this developmental stage. These findings are in full agreement with previously reported data (30). As evident from the present study (images in Fig. 5), the proposed interrelationship between nestin- and GC-B-expressing cells seems to concern these areas rather than the periventricular zone. Moreover, it can be proposed that the transient increase in nestin expression between E20 and P1 takes place in these areas.

The identification of GC-B coexpression with NeuN revealed that GC-B expression at P1 marks neuronal cells. NeuN is expressed in postmitotic neurons and appears first when cells initiate cellular and morphological differentiation (19). Thus, GC-B expression may be a feature of early neuronal progeny of nestin$^+$ cells. Most remarkably, we recognized that GC-B expression in NeuN$^+$ cells was correlated with peculiarities in the intensity and subcellular distribution of NeuN IR. It has been suggested that the intensity of NeuN labeling can differ between individual cells in relation to their acute physiological state (19, 31). In addition, NeuN is not exclusively expressed in nuclei but also detectable in the cytoplasm (19, 32). Functional roles for NeuN protein in the nucleus and even more in the cytoplasm are not yet understood. Our present findings, indicating enhanced nuclear staining intensity and the appearance of perinuclear IR in those NeuN$^+$ cells that coexpress GC-B, are therefore remarkable. These properties may define an early neuronal cell population in which CNP-GC-B-cGMP signaling and yet enigmatic roles of NeuN contribute to a distinct activity status. Distinct periods (both pre- and postnatal) of neuron generation are established (33), and recent quantitative analyses of neurons and glia in the developing neocortex of mice revealed that the number of neurons increased up to 100% between birth and P16 (34).

Possible signaling activities for CNP

Evidence for cellular functions of CNP during processes of neurogenesis came from studies with olfactory neuronal precursors (15). CNP was found to block neurotrophin-induced proliferation of these cells and promote their survival and maturation. The CNP effects were mimicked by 8-bromo-cGMP but not ANP or BNP, verifying the specific involvement and activity of GC-B. Indicating potential molecular mechanisms involved, further studies showed that CNP lowers the neurotrophin-mediated expression of cyclin D1 and simultaneously induces different inhibitory cell cycle proteins, apparently correlating with the attainment of different maturational cell fates (35). Providing evidence for an additional role of CNP during neural development, which is related to patterning events, the peptide was found to increase in mouse embryonic hindbrain cultures the expression of the sonic hedgehog target gene gli-1 (13). Considering the compartmentalized manner of cGMP signaling (1), all these reported cellular effects of CNP are compatible with the major perikarya localization of GC-B elucidated in the present study.

Although histological abnormalities were not detected in the brain of GC-B knockout mice, these animals showed symptoms (self-clasping, priapism) of neuronal disorders (9). Close inspection of the dorsal root entry zone in mice with inactivated GC-B revealed that GC-B-cGMP signaling is critical for proper sensory axon bifurcation during nervous system development (14). Reduced amounts of dorsal root ganglion neurons were found in CNP knockout mice (36).

Conclusion

Perinatal and early postnatal neurogenesis, affecting many CNS regions including the cerebral cortex, contributes significantly to brain maturation (33, 34, 37, 38). The transition process from neural stem cells to fully differentiated neurons and glia cells involves a cascade of distinct steps and different subtypes of precursor cells that differ in morphology, marker protein expression and mitotic activity (20, 39). Our present findings provide evidence that GC-B expression specifically marks early neuronal progeny of nestin-expressing progenitor cells and suggest that CNP/GC-B/cGMP signaling controls perinatal stages of brain maturation. Neurological disorders in GC-B-deficient mice (9) suggest physiological importance. Our findings also uncover an example for discrete roles of GC-A and GC-B signaling in the same target organ.

Acknowledgments

We are grateful to Gabriela Krasteva for support in confocal microscopy and thank Susanne Giehler, Jörn Lübberstedt, and Sabine Tasch for technical assistance.

Address all correspondence and requests for reprints to: Dr. Dieter Müller, Institute of Anatomy and Cell Biology, Justus-Liebig-University, Aulweg 123, 35385 Giessen, Germany. E-mail: hans-dieter.mueller@anatomie.med.uni-giessen.de.

This work was supported by Grants SFB 547 C13 and KFO 181/1 from the Deutsche Forschungsgemeinschaft and Grant 01 KY 9103/0 from the Bundesministerium für Forschung und Technologie. Support was also provided by the Peptide Radioiodination Service Center (University of Mississippi).

Disclosure Summary: The authors have nothing to disclose.

References

1. **Kuhn M** 2009 Function and dysfunction of mammalian membrane guanylyl cyclase receptors: lessons from genetic mouse models and implications for human diseases. Handb Exp Pharmacol 191:47–69
2. **Potter LR, Abbey-Hosch S, Dickey DM** 2006 Natriuretic peptides, their receptors, and cyclic guanosine monophosphate-dependent signaling functions. Endocr Rev 27:47–72
3. **Koller KJ, Goeddel DV** 1992 Molecular biology of the natriuretic peptides and their receptors. Circulation 86:1081–1088
4. **Müller D, Middendorff R, Olcese J, Mukhopadhyay AK** 2002 Central nervous system-specific glycosylation of the type A natriuretic peptide receptor. Endocrinology 143:23–29
5. **Konrad EM, Thibault G, Schiffrin EL** 1992 Autoradiographic visualization of the natriuretic peptide receptor-B in rat tissues. Regul Pept 39:177–189
6. **De Léan A, Racz K, Gutkowska J, Nguyen TT, Cantin M, Genest J** 1984 Specific receptor-mediated inhibition by synthetic atrial natriuretic factor of hormone-stimulated steroidogenesis in cultured bovine adrenal cells. Endocrinology 115:1636–1638
7. **Nikolaev VO, Gambaryan S, Engelhardt S, Walter U, Lohse MJ** 2005 Real-time monitoring of the PDE2 activity of live cells: hormone-stimulated cAMP hydrolysis is faster than hormone-stimulated cAMP synthesis. J Biol Chem 280:1716–1719
8. **Chusho H, Tamura N, Ogawa Y, Yasoda A, Suda M, Miyazawa T, Nakamura K, Nakao K, Kurihara T, Komatsu Y, Itoh H, Tanaka K, Saito Y, Katsuki M, Nakao K** 2001 Dwarfism and early death in mice lacking C-type natriuretic peptide. Proc Natl Acad Sci USA 98:4016–4021
9. **Tamura N, Doolittle LK, Hammer RE, Shelton JM, Richardson JA, Garbers DL** 2004 Critical roles of the guanylyl cyclase B receptor in endochondral ossification and development of female reproductive organs. Proc Natl Acad Sci USA 101:17300–17305
10. **Cao LH, Yang XL** 2008 Natriuretic peptides and their receptors in the central nervous system. Prog Neurobiol 84:234–248
11. **Gutkowska J, Antunes-Rodrigues J, McCann SM** 1997 Atrial natriuretic peptide in brain and pituitary gland. Physiol Rev 77:465–515
12. **Waschek JA** 2004 Developmental actions of natriuretic peptides in the brain and skeleton. Cell Mol Life Sci 61:2332–2342
13. **DiCicco-Bloom E, Lelièvre V, Zhou X, Rodriguez W, Tam J, Waschek JA** 2004 Embryonic expression and multifunctional actions of the natriuretic peptides and receptors in the developing nervous system. Dev Biol 271:161–175
14. **Schmidt H, Stonkute A, Jüttner R, Schäffer S, Buttgereit J, Feil R, Hofmann F, Rathjen FG** 2007 The receptor guanylyl cyclase Npr2 is essential for sensory axon bifurcation within the spinal cord. J Cell Biol 179:331–340
15. **Simpson PJ, Miller I, Moon C, Hanlon AL, Liebl DJ, Ronnett GV** 2002 Atrial natriuretic peptide type C induces a cell-cycle switch from proliferation to differentiation in brain-derived neurotrophic factor- or nerve growth factor-primed olfactory receptor neurons. J Neurosci 22:5536–5551
16. **Ryan MC, Gundlach AL** 1998 Ontogenic expression of natriuretic peptide mRNAs in postnatal rat brain: implications for development? Brain Res Dev Brain Res 105:251–268
17. **Lendahl U, Zimmerman LB, McKay RD** 1990 CNS stem cells express a new class of intermediate filament protein. Cell 60:585–595
18. **Encinas JM, Enikolopov G** 2008 Identifying and quantitating neural stem and progenitor cells in the adult brain. Methods Cell Biol 85:243–272
19. **Mullen RJ, Buck CR, Smith AM** 1992 NeuN, a neuronal specific nuclear protein in vertebrates. Development 116:201–211
20. **Mignone JL, Kukekov V, Chiang AS, Steindler D, Enikolopov G** 2004 Neural stem and progenitor cells in nestin-GFP transgenic mice. J Comp Neurol 469:311–324
21. **Middendorff R, Müller D, Mewe M, Mukhopadhyay AK, Holstein AF, Davidoff MS** 2002 The tunica albuginea of the human testis is characterized by complex contraction and relaxation activities regulated by cGMP. J Clin Endocrinol Metab 87:3486–3499
22. **Müller D, Olcese J, Mukhopadhyay AK, Middendorff R** 2000 Guanylyl cyclase-B represents the predominant natriuretic peptide receptor expressed at exceptionally high levels in the pineal gland. Mol Brain Res 75:321–329
23. **Müller D, Mukhopadhyay AK, Speth RC, Guidone G, Potthast R, Potter LR, Middendorff R** 2004 Spatiotemporal regulation of the two atrial natriuretic peptide receptors in testis. Endocrinology 145:1392–1401
24. **Davidoff MS, Middendorff R, Enikolopov G, Riethmacher D, Holstein AF, Müller D** 2004 Progenitor cells of the testosterone-producing Leydig cells revealed. J Cell Biol 167:935–944
25. **Thibault G, Grove KL, Deschepper CF** 1995 Reduced affinity of iodinated forms of Tyr^0 C-type natriuretic peptide for rat natriuretic peptide receptor B. Mol Pharmacol 48:1046–1053
26. **Müller D, Cortes-Dericks L, Budnik LT, Brunswig-Spickenheier B, Pancratius M, Speth RC, Mukhopadhyay AK, Middendorff R** 2006 Homologous and lysophosphatidic acid (LPA)-induced desensitization of the atrial natriuretic peptide receptor, guanylyl cyclase-A, in MA-10 Leydig cells. Endocrinology 147:2974–2985
27. **Bredt DS, Snyder SH** 1994 Transient nitric oxide synthase neurons in embryonic cerebral cortical plate, sensory ganglia, and olfactory epithelium. Neuron 13:301–313
28. **Sahlgren CM, Pallari HM, He T, Chou YH, Goldman RD, Eriksson JE** 2006 A nestin scaffold links Cdk5/p35 signaling to oxidant-induced cell death. EMBO J 25:4808–4819
29. **Kachinsky AM, Dominov JA, Miller JB** 1995 Intermediate filaments in cardiac myogenesis: nestin in the developing mouse heart. J Histochem Cytochem 43:843–847
30. **Zimmerman L, Parr B, Lendahl U, Cunningham M, McKay R, Gavin B, Mann J, Vassileva G, McMahon A** 1994 Independent regulatory elements in the nestin gene direct transgene expression to neural stem cells or muscle precursors. Neuron 12:11–24
31. **Weyer A, Schilling K** 2003 Developmental and cell type-specific expression of the neuronal marker NeuN in the murine cerebellum. J Neurosci Res 73:400–409
32. **Lind D, Franken S, Kappler J, Jankowski J, Schilling K** 2005 Characterization of the neuronal marker NeuN as a multiply phosphorylated antigen with discrete subcellular localization. J Neurosci Res 79:295–302
33. **Mooney SM, Miller MW** 2007 Postnatal generation of neurons in the ventrobasal nucleus of the rat thalamus. J Neurosci 27:5023–5032
34. **Lyck L, Krøigård T, Finsen B** 2007 Unbiased cell quantification reveals a continued increase in the number of neocortical neurones during early post-natal development in mice. Eur J Neurosci 26:1749–1764
35. **Simpson PJ, Moon C, Kleman AM, Connolly E, Ronnett GV** 2007 Progressive and inhibitory cell cycle proteins act simultaneously to regulate neurotrophin-mediated proliferation and maturation of neuronal precursors. Cell Cycle 6:1077–1089
36. **Kishimoto I, Tokudome T, Horio T, Soeki T, Chusho H, Nakao K, Kangawa K** 2008 C-type natriuretic peptide is a Schwann cell-derived factor for development and function of sensory neurones. J Neuroendocrinol 20:1213–1223
37. **Wei LC, Shi M, Chen LW, Cao R, Zhang P, Chan YS** 2002 Nestin-containing cells express glial fibrillary acidic protein in the proliferative regions of central nervous system of postnatal developing and adult mice. Brain Res Dev Brain Res 139:9–17
38. **Ganat YM, Silbereis J, Cave C, Ngu H, Anderson GM, Ohkubo Y, Ment LR, Vaccarino FM** 2006 Early postnatal astroglial cells produce multilineage precursors and neural stem cells *in vivo*. J Neurosci 26:8609–8621
39. **Götz M, Huttner WB** 2005 The cell biology of neurogenesis. Nat Rev Mol Cell Biol 6:777–788